

# Analysis of structural relaxation in a $\text{Li}_2\text{O}2\text{SiO}_2$ glass using rate heating approach

YANCHUN HAN\*

*Changchun Institute of Applied Chemistry, Chinese Academy of Sciences,  
Changchun 130022, Peoples Republic of China*

A. D'AMORE, L. NICOLAIS

*Department of Materials and Production Engineering, University of Naples Federico II,  
Piazzale Tecchio, 80125 Naples, Italy*

The structural relaxation process of an inorganic glass ( $\text{Li}_2\text{O}2\text{SiO}_2$ ) at different cooling rates has been studied by differential scanning calorimetry. A four-parameter model – Tool-Narayanaswamy-Moynihan (TNM) model was applied to simulate the normalized specific heat curve measured. Four parameters,  $\Delta h^*/R$ ,  $\beta$ ,  $\ln A$ , and  $x$  were obtained and compared with the values obtained from the isothermal approach. © 1999 Kluwer Academic Publishers

## 1. Introduction

Over the years there has been a growing interest in the structural relaxation and recovery processes observed in glassy materials of all kinds, including molecular (organic) [1, 2], inorganic [3–5], polymeric [6–9], and metallic glasses [10–12]. The nature of the problem is clearly related to the intrinsic properties of the “ill-condensed”, i.e., nonequilibrium, glassy state, as each of the above classes of materials shows remarkably similar structural relaxation behavior despite obvious differences in the chemical moieties and in the nature of the molecular or atomic forces involved.

Structural relaxation is a result of the nonequilibrium nature of the glassy state, which spontaneously evolves toward some equilibrium state (defined by  $T$  and  $P$ ) at a rate that depends on the temperature, the pressure, and the complete thermomechanical history of the glass. This fact has long been recognized, and a large amount of experimental and theoretical work has been aimed at understanding the observed phenomena.

In the past two decades, researchers have proposed various phenomenological models [13–17] to describe the structural relaxation phenomenon. A comprehensive review of those models is contained in a recently published book [18] and will not be repeated here. A phenomenological model describes the change of a certain property but does not provide a theoretical explanation for the observation. Instead, it serves an intermediate role, as it concisely presents the experimental data and provides a starting point for the development of a theory.

Enthalpy relaxation can be studied with DSC using either the rate heating approach or the isothermal approach. The rate heating approach, in which the specimen is cooled through the glass transition region and immediately heated back to the rubbery

state, reveals the temperature dependence of the enthalpy relaxation and it focuses on the effect of cooling (and/or heating) on the specific heat function in the glass transition range. The isothermal approach, which includes an isothermal period between cooling and heating, demonstrates both temperature and structure dependence of relaxation. Also, in the isothermal approach, substantial structural change occurs during the isothermal period. Both approaches have been applied to study various glasses in the past. The rate heating approach was used to study relaxation in several alkali glasses [13], a chalcogenide glass [3], a boron oxide glass [14], an organic molecule (5-phenyl-4-ether) [3], and a fluoride glass [19]. Sasabe and coworkers applied the rate heating approach in their studies of soda-lime silica glass [20], and poly(vinyl acetate) [21]. Gonchukova employed the rate heating approach to study a glass composed of 60% PbO and 40%  $\text{SiO}_2$  [22]. Gonchukova and Mazurin also investigated a metallic glass, SiCuPd [23]. The isothermal approach was used by Chen to study PdNiP glass [24], and by Chen and Kurkjian to study a boron oxide glass [25].

In this paper, the rate heating approach was employed to study the structural relaxation process in an inorganic glass ( $\text{Li}_2\text{O}2\text{SiO}_2$ ). The Tool-Narayanaswamy-Moynihan model was used to simulate the experimental data. The results obtained from the rate heating approach were compared with those obtained from the isothermal approach.

## 2. Tool-Narayanaswamy-Moynihan model

The model is based on an equation for fictive temperature (proposed by Tool [26]) in the form written by Moynihan [13, 14] and an equation for structural relaxation time due to Narayanaswamy [16]. The two

\* Author to whom all correspondence should be addressed.

equations are coupled and the model is referred to as the Tool-Narayanaswamy-Moynihan (TNM) model.

The fictive temperature,  $T_f$ , is the temperature at which a nonequilibrium glass at temperature  $T$  would be in equilibrium. The mathematical definition of fictive temperature is:

$$\int_T^{T_0} [\partial(P - P_g)/\partial T] dT = \int_{T_f}^{T_0} [\partial(P_e - P_g)/\partial T] dT \quad (1)$$

where  $P$  denotes a structure sensitive property (such as enthalpy or volume) and the subscripts  $e$  and  $g$  refer to equilibrium and glassy state, respectively.  $T$  is the actual temperature,  $T_0$  is the temperature in the equilibrium rubbery state, and  $T_f$  is the fictive temperature. Taking the derivative with respect to temperature on both sides of Equation 1, we obtain:

$$dT_f/dT = [R(T) - R_g(T)]/[R_e(T_f) - R_g(T_f)] \quad (2)$$

where  $R$  is the temperature derivative of  $P$  and the subscripts are previously defined.

When enthalpy is the measured structure sensitive property, its temperature derivative is specific heat and Equation 2 becomes:

$$C_p^N(T) = [C_p(T) - C_{pg}(T)]/[C_{pe}(T_f) - C_{pg}(T_f)] \quad (3)$$

The normalized specific heat,  $C_p^N$ , is experimentally determined by DSC and is related to the temperature derivative of fictive temperature. This is obvious when Equations 2 and 3 are compared. The variation of the normalized specific heat during structural relaxation is described by a relaxation function  $\Phi(t)$ . The most widely used relaxation function is the so-called stretched exponential or Kohlrausch-Williams-Watts (KWW) [27] equation, which is related to the structural sensitive property  $P$  according to the following equation:

$$\Phi(t) = \frac{P - P_e}{P_0 - P_e} = \exp \left[ - \left( \int_{t_1}^t dt'/\tau \right)^\beta \right] \quad (4)$$

In Equation 4,  $t_1$  is the time when the change in temperature occurs,  $\beta$  is the KWW exponent, and  $\tau$  is the characteristic relaxation time. Nonexponentiality is reflected in the value of  $\beta < 1$ . When treating nonisothermal situations (arbitrary thermal history) one assumes that the relaxation function can be represented by the superposition of responses to a series of temperature jumps that constitute the thermal history. The fictive temperature then takes on the following form:

$$T_f(T) = T_0 + \int_{T_0}^T dT' \left\{ 1 - \exp \left[ - \left( \int_{t(T')}^{t(T)} dt'/\tau \right)^\beta \right] \right\} \quad (5)$$

where  $T_0$  is the initial temperature.

The next input needed in the model is an expression for the structural relaxation time  $\tau$ , which appears in Equation 5. Following Tool's original work, various expressions for the structural relaxation time have been proposed, all exponential in the form and containing temperature and fictive temperature as variables. In this study we select the Narayanaswamy-Moynihan (NM) expression:

$$\tau = A \exp[X\Delta h^*/RT + (1 - X)\Delta h^*/RT_f] \quad (6)$$

where  $T$  and  $T_f$  are previously defined and  $\tau$  is the structural relaxation time. Nonlinearity parameter  $x$  ( $0 < x < 1$ ) partitions the activation energy  $\Delta h^*$  into two parts that characterize the relative effects of temperature and structural, respectively, on the relaxation time.

The modeling strategy can be summarized as follows: fictive temperature is related to a structure sensitive property,  $P$ , and the normalized relaxation function,  $\Phi(t)$ , according to Equations 2–4, and as such can be experimentally determined. The simulated relaxation can be obtained by solving Equations 5 and 6 simultaneously and verified against the experimental results.

### 3. Optimization of model parameters

To accommodate the discrete nature of numerical calculations, we begin by rewriting Equations 5 and 6 as follows:

$$T_f(m) = T_0 + \sum_{j=1}^m \Delta T(j) \left\{ 1 - \exp \left[ - \left( \sum_{k=j}^m \Delta t(k)/\tau(k) \right)^\beta \right] \right\} \quad (7)$$

and

$$\tau(k) = A \exp\{X\Delta h^*/[RT(k)] + (1 - X)\Delta h^*/[RT_f(k)]\} \quad (8)$$

In Equation 7 and 8,  $m$  is an iteration index, and  $j$  and  $k$  are dumb indices. A caution must be exercised in that  $T_0$ , the starting temperature for the simulation, must be sufficiently high, so that the system is initially in equilibrium at that temperature. This is a necessary condition since the properties of glasses are route dependent, and every step in the thermal history continues to affect their current response. For simple thermal histories the conversion from continuous to discrete form can be performed in a straight forward manner.

Finally, the temperature derivative of the fictive temperature in the  $i$ th interval during cooling or heating can be approximated by:

$$dT_{f(i)}/dT = [T_{f(i+1)} - T_{f(i)}]/[T_{(i+1)} - T_i] \quad (9)$$

From Equations 7 to 8, the model yields the  $T_f$  of the system as a function of the thermal history, while from

Equation 9 one obtains the temperature derivative of the fictive temperature. The latter is related to the relaxing property, such as the volume in the case of volume relaxation or enthalpy in the case of enthalpy relaxation, by Equation 2. In this manner it is possible to compare the model prediction with the experimental results and hence check the validity and accuracy of the model.

The goal of our optimization procedure is to best describe the specific heat of the sample in the glass transition region. The object function for optimization is  $\sum(C_p^{N^*} - C_p^N)^2$ , where  $C_p^{N^*}$  is the calculated value of the normalized specific heat in the transition region and  $C_p^N$  is its experimentally obtained counterpart. Optimization was carried out using the Marquardt algorithm given by Kuester and Mize [28] which, with a proper choice of starting values, converges in the written in Fortran and could be accommodated and executed in a personal computer.

#### 4. Experimental

A sample of 14.00 mg  $\text{Li}_2\text{O}_2\text{SiO}_2$  was sealed in aluminum pan and used in all measurements. A differential scanning calorimeter, Mettler DSC 30, was used to perform thermal analysis and a general procedure was used:

1. Heating the sample to temperature ( $T_0 = 788$  K) between the glass transition and onset of crystallization temperatures and keep at this temperature for at least 10 min in order to erase the effects of the previous history.
2. Quenching the sample to the temperature  $T_1 = 623$  K at different quenching rates (0.5, 2.5, 5, 10, 20, 40, 80 °C/min).
3. Scanning the sample at a heating rate of 10 °C/min from the  $T_1$  to  $T_0$  and collecting the data.

For convenience, the thermal history will be referenced to as  $-0.5/10$ , with appropriate changes for other cooling rates.

#### 5. Results and discussion

Fig. 1 shows the effect of cooling rate on the heat capacity ( $C_p$ ) of  $\text{Li}_2\text{O}_2\text{SiO}_2$  in the glass transition. The sample was cooled at different rates from the equilibrium liquid state to the glassy state before heating at 10 °C/min. The biggest endothermic peak is at a cooling rate of 0.5 °C/min. The decrease in the endotherm with increased cooling rate can be clearly observed.

The integration of  $C_p$  from the glassy state to the equilibrium liquid establishes the relative enthalpy of the glass. This permits the evaluation of frozen-in fictive temperature  $T_f'$  of the glass. Fig. 2 shows the corresponding Arrhenius plot of cooling rate  $Q_c$  versus the frozen-in fictive temperature  $T_f'$ . As explained in [15], the slope of this plot gives the average activation energy  $\Delta h^*$  controlling structural relaxation very close equilibrium in the glass transition region:

$$\Delta h^*/R = -d \ln Q_c / d(1/T_f') \quad (10)$$

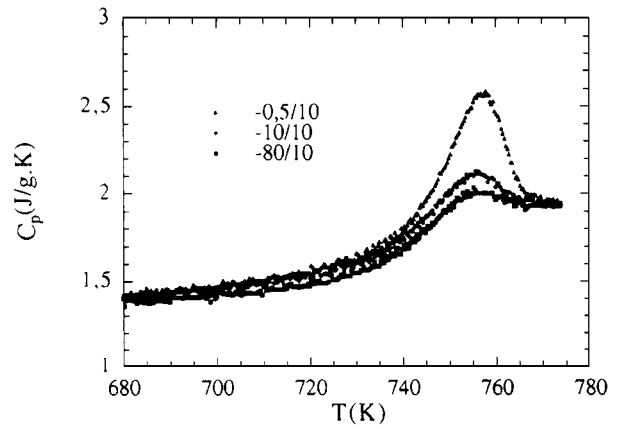


Figure 1 Heat capacities of a  $\text{Li}_2\text{O}_2\text{SiO}_2$  glass measured at a heating rate of 10 °C/min immediately following a cooling at a rate of 0.5, 10, and 80 °C/min.

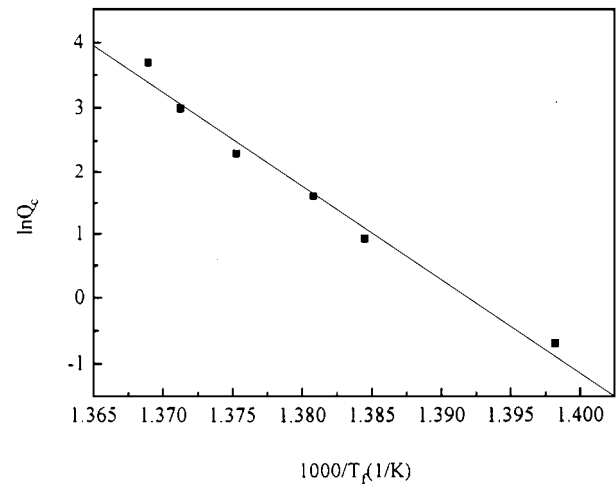


Figure 2 Arrhenius plot of logarithm of cooling rate vs. reciprocal of fictive temperature for a  $\text{Li}_2\text{O}_2\text{SiO}_2$  glass.

where  $R$  is the ideal gas constant.  $\Delta h^*/R$  for the present  $\text{Li}_2\text{O}_2\text{SiO}_2$ , determined from the slope of the line in Fig. 2, is  $155.89 \times 10^3$  K.

#### 6. Optimization of model parameters

The specific heat was then normalized according to Equation 3. We began our optimization process by obtaining a set of starting values for  $\text{Li}_2\text{O}_2\text{SiO}_2$ . We determined the starting values for the parameters in the following way:

1.  $\Delta h^*/R$  was obtained experimentally from the dependence of the frozen in fictive temperature  $T_f'$  on the cooling rate  $Q_c$ , which is  $155.89 \times 10^3$  K.
2.  $\ln A$  was determined from Equation 6 by assuming that at the glass transition temperature  $\tau$  is of order of 1 min and  $T = T_f' (=T_g)$ . With  $T_g = 733$  K and  $\Delta h^*/R$  obtained in step 1,  $\ln A$  is  $-213$ , which can be calculated from

$$\ln A = -\Delta h^*/(RT_g) \quad (11)$$

3.  $x$  and  $\beta$  were chosen to be in agreement with literature values reported by many researchers [6–9]. We chose  $x = 0.3$ ,  $\beta = 0.5$  as initial values.

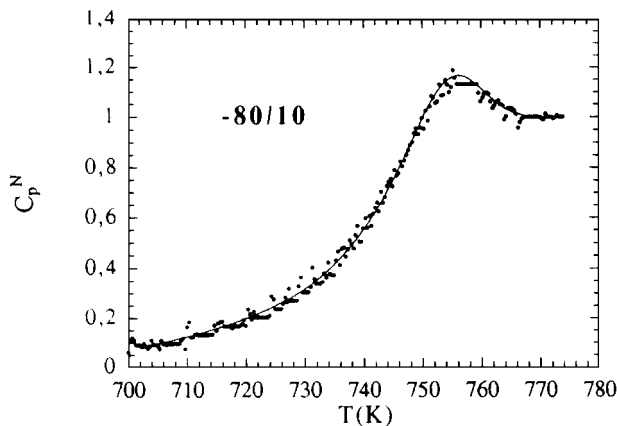


Figure 3 Experimental points and fits (solid line) for  $C_p^N$  as a function of cooling rate for a  $\text{Li}_2\text{O}_2\text{SiO}_2$  glass. Best fit parameters are given in Table I.

The other parameters in the simulation were set according to the experimental conditions, namely,  $T_0 = 773$  K,  $T_1 = 700$  K. A preliminary calculation of the  $C_p^N$  was then performed with these values. The chosen values of the order parameters were first put into Equation 8 to calculate  $\tau$  which was then used in Equation 7 to calculate  $T_f$ . The value of  $dT_f/dT$  or  $C_p^N$  was then evaluated using Equation 9. The values of the order parameters were adjusted to minimize the deviation, namely  $\sum(C_p^{N*} - C_p^N)^2$ , and the above calculations were repeated. The optimized parameters were usually arrived at after about 15–20 iterations, but because of the repetitive nature of the calculation, it took 2–3 h to perform calculations in a personal computer.

Fig. 3 compares a few experimental and calculated curves; the examples are typical of the general trends in the results. Each curve representing a given cooling rate is fit to the model individually by using the aforementioned optimization routine. In all the cases examined so far, the calculated curves are reasonably good approximations to the experimental data; the model accurately indicates the position and the width of the glass transition region. The optimized parameters are given in Table I.

In the following figures the effect of cooling rate on the calculated optimized model parameters ( $\Delta h^*/R$ ,  $\beta$ ,  $\ln A$ , and  $x$ ) is shown. We saw in Figs 4 and 5 that the activation energy and  $\ln A$  are nearly independent of cooling rate within experimental error. The average values of  $\Delta h^*/R$  and  $\ln A$  are  $132.80 \times 10^3$  K and  $-178.71$ , respectively. A comparison of  $\Delta h^*/R$  and  $\ln A$  obtained from rate heating approach and isothermal approach was shown in Table II.

TABLE I  $\Delta h^*/R$ ,  $\beta$ ,  $\ln A$ , and  $x$  as a function of cooling rate for a  $\text{Li}_2\text{O}_2\text{SiO}_2$  glass

$Q_c$ ( $^\circ\text{C}/\text{min}$ )	$\Delta h^*/R$ ( $\times 10^3$ K)	$\ln A$	$\beta$	$x$
0.5	133.87	-180.61	0.31	0.11
2.5	128.52	-173.19	0.38	0.13
5	123.58	-166.57	0.39	0.11
10	125.09	-168.41	0.46	0.20
20	122.39	-164.70	0.47	0.15
40	142.96	-191.91	0.45	0.04
80	153.17	-205.60	0.48	0.04

TABLE II A comparison of  $\Delta h^*/R$  and  $\ln A$  obtained from different method for a  $\text{Li}_2\text{O}_2\text{SiO}_2$  glass

Method	$\Delta h^*/R$ ( $\times 10^3$ K)	$\ln A$
Cooling	155.89	-213.00
Rate heating approach	132.80	-178.71
Isothermal approach	116.62	-150.02

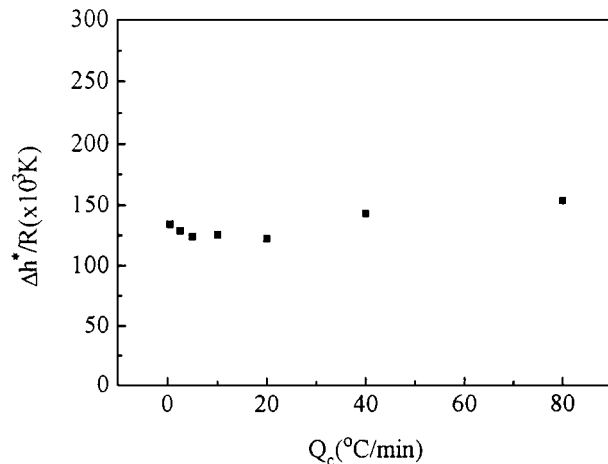


Figure 4  $\Delta h^*/R$  as a function of cooling rate for a  $\text{Li}_2\text{O}_2\text{SiO}_2$  glass.

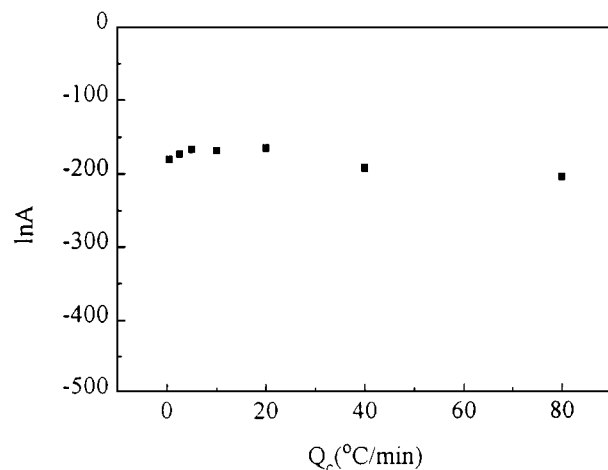


Figure 5  $\ln A$  as a function of cooling rate for a  $\text{Li}_2\text{O}_2\text{SiO}_2$  glass.

From Fig. 6 we can see that  $\ln A$  is directly proportional to  $\Delta h^*/R$ . This verified the validity of Equation 11 from experiments.

$\beta$  is an empirical measure of the width of the distribution of relaxation times. From Fig. 7 we can see that when the cooling rate is below  $10^\circ\text{C}/\text{min}$ ,  $\beta$  increases with increasing cooling rate; when the cooling rate is above  $10^\circ\text{C}/\text{min}$ ,  $\beta$  nearly keep constant and is in the range of 0.47. This is nearly the same with the value ( $\beta = 0.49$ ) obtained from the isothermal approach.

The partitioning parameter  $x$  is empirically defined as the fraction of the relaxation time that is due solely to the absolute temperature of the system; its complement,  $(1 - x)$ , defines that part of the relaxation time that is determined by the instantaneous state of the system as reflected in the fictive temperature. Fig. 8 shows the result of  $x$  as a function of cooling rate. At the cooling rate below  $10^\circ\text{C}/\text{min}$ ,  $x$  increases with increasing cooling

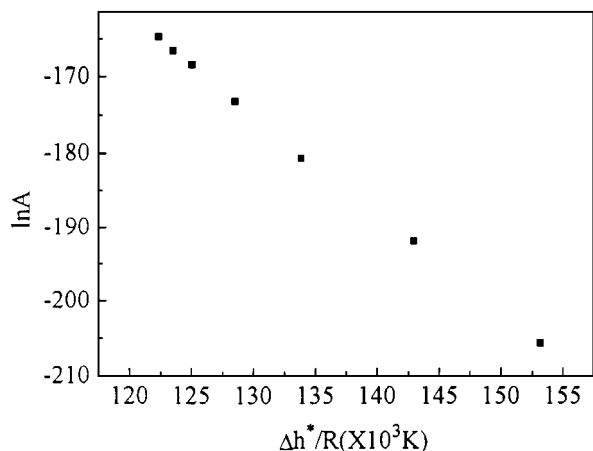


Figure 6 The relationship between  $\Delta h^*/R$  and  $\ln A$  for a  $\text{Li}_2\text{O}_2\text{SiO}_2$  glass.

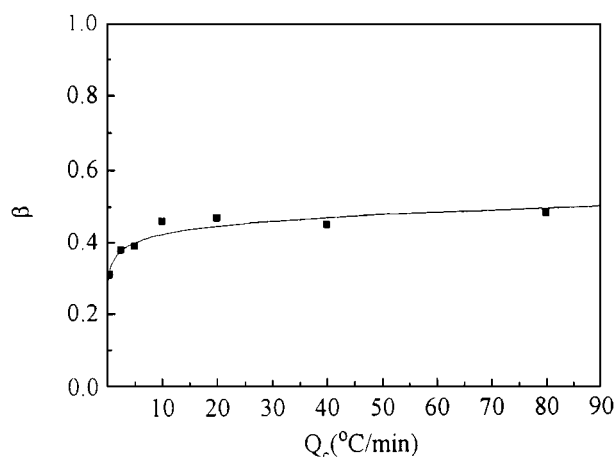


Figure 7  $\beta$  as a function of cooling rate for a  $\text{Li}_2\text{O}_2\text{SiO}_2$  glass.

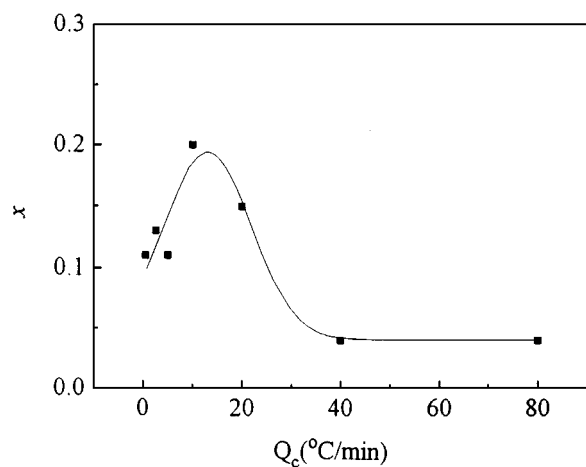


Figure 8  $x$  as a function of cooling rate for a  $\text{Li}_2\text{O}_2\text{SiO}_2$  glass.

rate. But when the cooling rate is above  $10\text{ }^\circ\text{C}/\text{min}$ ,  $x$  decreases with increasing cooling rate. When the cooling rate is higher than  $40\text{ }^\circ\text{C}/\text{min}$ ,  $x$  nearly keeps constant and is very small. As we know that  $x$  is a term describing the relative effects of temperature and structure on the rate of relaxation. The smaller  $x$ , the less relaxation time dependence on temperature. From the isothermal approach we knew that  $x$  is a function of ageing time

and temperature. So the values of  $x$  obtained from these two different methods can not be compared.

In some cases the parameters obtained for the unannealed samples do not follow the same trend as the annealed samples; this is true even though the model can predict these curves very accurately, owing to their relatively simple shape. It is not clear whether this represents an artifact of the analysis or is an intrinsic deficiency of the model; in rare instances this is not observed, which suggests that the effect is real.

## 7. Conclusions

The structural relaxation process of an inorganic glass ( $\text{Li}_2\text{O}_2\text{SiO}_2$ ) at different cooling rates has been studied by differential scanning calorimetry. A four-parameter model – Tool-Narayanaswamy-Moynihan (TNM) model was applied to simulate the normalized specific heat curve measured. Four parameters,  $\Delta h^*/R$ ,  $\beta$ ,  $\ln A$ , and  $x$  were obtained and compared with the values obtained from the isothermal approach. The calculated curves are reasonably good approximations to the experimental data. The model accurately indicates the position and the width of the glass transition region, i.e. the glass transition phenomenon of the  $\text{Li}_2\text{O}_2\text{SiO}_2$  glass.

## Acknowledgements

It is a pleasure to thank Dr. G. Carotenuto and A. Visconti of University of Naples, for their assistance with the experiments and Dr. Yuming Yang of Changchun Institute of Applied Chemistry, Chinese Academy of Sciences, for valuable and stimulating discussions.

## References

1. L. C. E. STRUIK, "Physical Ageing in Amorphous Polymers and Other Materials" (Elsevier, Amsterdam, 1978).
2. A. S. MARSHALL and S. E. B. PETRIE, *J. Appl. Phys.* **46** (1975) 4224.
3. C. T. MOYNIHAN, P. B. MACEDO, C. J. MONTROSE, P. K. GUPTA, M. A. DEBOLT, J. F. DILL, B. E. DOM, P. W. DRAKE, A. J. EASTEAL, P. B. ELTERMAN, R. A. MOELLER, H. SASABE and J. A. WILDER, *Ann. N.Y. Acad. Sci.* **279** (1976) 15.
4. H. S. CHEN and C. R. KURKJIAN, *J. Amer. Ceram. Soc.*, **66** (1983) 613.
5. A. BARKATT and C. A. ANGELL, *J. Phys. Chem.* **82** (1978) 1972.
6. A. R. BERENS and I. M. HODGE, *Macromolecules* **15** (1982) 756.
7. I. M. HODGE and A. R. BERENS, *ibid.* **15** (1982) 762.
8. I. M. HODGE and G. S. HUVARD, *ibid.* **16** (1983) 371.
9. I. M. HODGE, *ibid.* **16** (1983) 898.
10. H. S. CHEN, *J. Appl. Phys.* **52** (1981) 1868.
11. A. L. GREER and F. SPAEPEN, *Ann. NY Acad. Sci.* **371** (1981) 218.
12. T. EGAMI, *ibid.* **371** (1981) 238.
13. C. T. MOYNIHAN, A. J. EASTEAL, M. A. DEBOLT and J. TUCKER, *J. Amer. Ceram. Soc.* **59** (1976) 12.
14. M. A. DEBOLT, A. J. EASTEAL, P. B. MACEDO and C. T. MOYNIHAN, *ibid.* **59** (1976) 16.
15. A. J. KOVACS, *et al.*, *J. Polym. Sci., Polym. Phys. Ed.* **17** (1979) 1097.
16. O. S. NARAYANASWAMY, *J. Amer. Ceram. Soc.* **54** (1971) 491.

17. J. M. HUTCHINSON, A. J. KOVACS, *J. Polym. Sci., Polym. Phys. Ed.* **14** (1976) 1575.
18. G. SHERER, "Relaxation in Glass and Composites" (Wiley, New York, 1986).
19. C. T. MOYNIHAN, A. J. BRUCE, D. L. GAVIN, S. R. LOEHR, S. M. OPALKA and M. G. DREXHAGE, *Polym. Eng. Sci.* **24** (1984) 1117.
20. H. SASABE, M. A. DeBOLT, P. MACEDO and C. T. MOYNIHAN, in Proceedings of the 11th International Congress of Glass, Prague, Czechoslovakia (1977).
21. H. SASABE and C. T. MOYNIHAN, *J. Polym. Sci.* **16** (1978) 1667.
22. N. O. GONCHUKOVA, *Sov. J. Glass Phys. Chem.* **7** (1981) 217.
23. N. O. GONCHUKOVA and O. V. MAZURIN, *Acad. Sci. USSR Proc. Chem. Sec.* **270** (1983) 1137.
24. H. S. CHEN, *J. Non-Cryst. Sol.* **46** (1981) 289.
25. H. S. CHEN and C. R. KURKJIAN, *J. Amer. Ceram. Soc.* **66** (1983) 613.
26. A. Q. TOOL, *ibid.* **29** (1946) 240.
27. G. WILLIAMS, D. C. WATTS, *Trans. Faraday Soc.* **66** (1970) 80.
28. J. L. KUESTER and J. H. MIZE, "Optimization Techniques with FORTRAN" (McGraw-Hill, New York, 1973).

*Received 19 May 1997  
and accepted 8 October 1998*